Activation of Metabotropic Glutamate Receptor 5 Modulates Microglial Reactivity and Neurotoxicity by Inhibiting NADPH Oxidase*

David J. Loane[1], Bogdan A. Stoica, Ahdeah Pajoohesh-Ganji, Kimberly R. Byrnes, and Alan I. Faden
From the Department of Neuroscience, Georgetown University Medical Center, Washington, D. C. 20057

Microglial-related factors have been implicated in the signaling cascades that contribute to neuronal cell death in various neurodegenerative disorders. Thus, strategies that reduce microglial activation and associated neurotoxicity may have therapeutic benefit. Group II and III metabotropic glutamate receptors (mGluRs) are expressed in microglia and can modulate microglial activity in primary cell cultures. We demonstrate that the group I receptor member mGluR5 is highly expressed in primary microglial cultures and the BV2 microglial cell line. Activation of mGluR5 using the selective agonist (RS)-2-chloro-5-hydroxyphenylglycine (CHPG) significantly attenuates microglial activation in response to lipopolysaccharide and interferon-γ, as indicated by a reduction in the expression of inducible nitric-oxide synthase, production of nitric oxide and tumor necrosis factor-α, and intracellular generation of reactive oxygen species. In addition, microglial-induced neurotoxicity is also markedly reduced by CHPG treatment. The anti-inflammatory effects of CHPG are mediated by the mGluR5 receptor, because either a selective mGluR5 antagonist or small interference RNA knockdown attenuated the actions of this drug. CHPG blocked the lipopolysaccharide-induced increase in expression and enzymatic activity of NADPH oxidase. Moreover, the protective effects of CHPG were significantly reduced when the NADPH oxidase subunits $p22^{phox}$ or $gp91^{phox}$ were knocked down by small interference RNA. These data suggest that mGluR5 represents a novel target for modulating microglial-dependent neuroinflammation, and may have therapeutic relevance for neurological disorders that exhibit microglial-mediated neurodegeneration.

A prominent feature of many neurological disorders such as Alzheimer disease, Parkinson disease, multiple sclerosis, AIDS-associated dementia, or brain trauma, is a prolonged localized inflammatory response that contributes to the progressive loss of neurons in discrete areas of the central nervous system (1). Microglia, the resident immune cells in the brain, are highly responsive to environmental stresses or immunological challenges and have been implicated as the predominant cell type governing inflammation-mediated neuronal damage (2). In particular, activated microglia exert neurotoxic effects by releasing inflammatory mediators such as eicosanoids, cytokines, chemokines, and reactive free radicals (3). Although these factors are necessary for immunological surveillance of the local brain environment, microglial responses must be tightly regulated so as to avoid over-activation and associated neurotoxic effects (3).

Microglia respond to toxic agents, such as the bacterial endotoxin lipopolysaccharide (LPS)[2] and cytokines (e.g. interferon-γ (IFNγ)), by releasing reactive oxygen species (ROS) (4, 5). NADPH oxidase is an enzyme complex that plays a key role in microglial production of ROS. The NADPH oxidase complex is composed of cytosolic subunits ($gp40^{phox}$, $p47^{phox}$, and $p67^{phox}$, and the GTP-binding protein p21-Rac1) and membrane subunits ($gp91^{phox}$ and $p22^{phox}$) (6). Upon activation, protein kinase C- and MAPK-mediated phosphorylation of the cytosolic subunits results in their translocation to the membrane where they assemble with membrane subunits to form the active NADPH oxidase (7–9). The active enzyme complex produces O^{2-}, which is converted into superoxide-derived oxidants such as H_2O_2, hydroxyl radicals, and peroxynitrite (10), which are highly neurotoxic (3, 4). In addition, ROS generation has important effects on microglia themselves, facilitating pro-inflammatory pathways by activating MAPK and NFκB signaling. The latter induces transcription of pro-inflammatory mediators such as iNOS, nitric oxide (NO), and tumor necrosis factor-α (TNFα); these factors induce a self-propagating cycle that causes prolonged microglial activation and neuroinflammation. Considerable evidence suggests that the over-activation of NADPH oxidase plays a key role in inflammation-mediated neurodegeneration and may therefore be an important target for therapeutic intervention (11, 12).

Metabotropic glutamate receptors (mGluRs) have been considered promising targets for neuroprotective drug discovery, and many studies have focused on modulating mGluR activity in neurons (13–16). However, mGluRs are also expressed on astrocytes (17, 18) and microglia (19, 20), although their roles in neuroinflammation have received limited attention to date.

---

[1] To whom correspondence should be addressed: Dept. of Neuroscience, Georgetown University Medical Center, 3970 Reservoir Rd, NW, Washington, D. C. 20057. Tel.: 202-784-9502; Fax: 202-687-0617; E-mail: djl42@georgetown.edu.

[2] The abbreviations used are: LPS, lipopolysaccharide; IFNγ, interferon γ; ROS, reactive oxygen species; MAPK, mitogen-activated protein kinase; iNOS, inducible nitric-oxide synthase; TNFα, tumor necrosis factor-α; mGluR, metabotropic glutamate receptor; CHPG, (RS)-2-chloro-5-hydroxyphenylglycine; MTEP, 3-[(2-methyl-1,3-thiazol-4-yl)ethynyl]pyridine; siRNA, small interference RNA; PBS, phosphate-buffered saline; PI, phosphoinositide; ANOVA, analysis of variance; H_2DCFDA, 2′,7′-dichlorodihydrofluorescein diacetate; CPCCOEt, 7-(hydroxyimino)cyclopropa[b]chromen-1a-carboxylate ethyl ester.

mGluRs are G-protein-coupled receptors that include at least eight subtypes, which have been classified into three groups based on their pharmacological profiles and signal transduction pathways. Stimulation of group II mGluRs (mGluR2 and -3) induce microglial activation, TNFα, and Fas ligand release, leading to mitochondrial depolarization and neuronal apoptosis (21, 22). In contrast, activation of microglial group III receptors (mGluR4, -6, and -8) may be protective (20). Of the group I receptors (mGluR1 and -5) only mGluR5 mRNA has been shown to be expressed in microglia (19); however, its functional role in microglial activation and neuroinflammation has not been examined.

In neurons, activation of mGluR5 can inhibit caspase-dependent neuronal apoptosis in cell culture models (23, 24), and although mGluR5 antagonists have been reported to be neuroprotective, such effects are unrelated to actions at the mGluR5 receptor (25). In contrast, activation of mGluR1 exacerbates neuronal cell death (23), whereas selective mGluR1 antagonists are neuroprotective *in vitro* and *in vivo* (16, 26, 27). Group I mGluRs are coupled to $G\alpha_q$-proteins/phospholipase C stimulation, causing increased inositol triphosphate and calcium release, and activation of protein kinase C. Although mGluR1 and mGluR5 share certain common signaling mechanisms, they have remarkably different profiles in central nervous system injury (23).

In this study, LPS and IFNγ models of microglial activation were used in BV2 and primary microglial cultures to investigate the impact of mGluR5 receptor activation on microglial reactivity and neurotoxicity. We show that microglia express functional mGluR5 receptors, which upon activation negatively regulate the release of microglial-associated inflammatory mediators and related neurotoxicity. Moreover, we demonstrate that the protective effects of microglial mGluR5 activation are mediated through the inhibition of the NADPH oxidase enzyme, and suggest that this novel strategy to reduce neuroinflammation may have therapeutic relevance for many neurological disorders that exhibit microglial-mediated neurodegeneration.

EXPERIMENTAL PROCEDURES

Microglial Cultures—Primary cortical microglial were obtained from postnatal day 2 Sprague-Dawley rat pups and cultured as described before (28). Briefly, the whole brain was carefully dissected and homogenized in L15 media (Invitrogen). Mixed glial cultures were incubated for 8–10 days at 37 °C with 5% CO_2 in Dulbecco's modified Eagle medium (Invitrogen) with 10% fetal calf serum (HyClone, Logan, UT), 1% L-glutamine (Invitrogen), 1% sodium pyruvate (Invitrogen), and 1% Pen/Strep (Fisher, Pittsburgh, PA). After the initial incubation, the cells were shaken for 1 h at 100 rpm and 37 °C. Detached microglia were collected and replated as purified cultures with greater than 96% purity. The BV2 murine microglial cell line was kindly provided by Dr. Carol Colton (Duke University Medical Center, Durham, NC). The cells were grown and maintained in Dulbecco's modified Eagle medium supplemented with 10% fetal bovine serum (HyClone) at 37 °C in a humidified incubator under 5% CO_2.

Drug Treatments—The mGluR5 agonist, CHPG ((RS)-2-chloro-5-hydroxyphenylglycine, 100 μM to 10 mM), group 1 mGluR agonist, DHPG ((RS)-3,5-dihydroxyphenylglycine, 50 μM), and the mGluR1 antagonist, CPCCOEt (7-(hydroxyimino)cyclopropa[b]chromen-1a-carboxylate ethyl ester, 100 μM, all from Tocris Bioscience, Ellisville, MO) were applied alone and/or in combination to microglia for 1 h prior to LPS (Sigma-Aldrich, 100 ng/ml) or recombinant mouse IFNγ (R&D Systems, Minneapolis, MN, 0.5 and 2 ng/ml) stimulation. The mGluR5 antagonist, MTEP (3-[(2-methyl-1,3-thiazol-4-yl)-ethynyl]pyridine, 10 μM), was a gift from Merck Research Laboratories (Rahway, NJ), and was administered 30 min prior to CHPG administration. All drugs were prepared and stored according to the manufacturer's guidelines.

RNA Interference—Small interfering RNA (siRNA) containing a mixture of three targeted siRNAs for mouse mGluR5, p22^{phox}, and gp91^{phox} were purchased from Santa Cruz Biotechnology (Santa Cruz, CA). BV2 microglia cultured in 24-well plates were transfected with the appropriate siRNA (100 nM) using Lipofectamine2000 (Invitrogen). After 24 h of transfection, cells were pre-treated with CHPG (4 mM) for 1 h, stimulated with LPS (100 ng/ml), and cultured for an additional 24 h. Control siRNA duplex containing scrambled sequences (Santa Cruz Biotechnology) was used in parallel experiments. Optimal transfection efficiency and conditions were determined by using fluorescein-labeled double strand RNA oligomers (BLOCK-iT Fluorscent Oligo, Invitrogen). The transfection efficiency of siRNA in BV2 microglia was ~50% as determined by fluorescently labeled cells containing the fluorescent-oligonucleotide siRNA 24 h after transfection (data not shown). Effective gene knockdown was analyzed by Western immunoblotting.

Immunocytochemistry—BV2 and primary cortical microglia were seeded onto poly-D-lysine-coated coverslips in 24-well plates at a density of 8×10^5 cells/well. After 24 h, cells were pre-treated for 1 h with CHPG, stimulated with LPS, and incubated for an additional 24 h. Cells were washed in warm PBS and fixed in 4% paraformaldehyde for 15 min followed by three washes with PBS for 10 min each. Cells were incubated in blocking buffer (10% normal goat serum in PBS containing 0.1% Triton X-100) for 2 h, followed by overnight incubation at 4 °C in primary antibody (mGluR5, 1:100 (Abcam, Cambridge, MA); ED1, 1:100 (AbD Serotec, Raleigh, NC); p22^{phox}, 1:50 (Santa Cruz Biotechnology); and gp91^{phox}, 1:100 (BD Transduction, Franklin Lakes, NJ)). The next day, cells were washed with PBS three times for 10 min, followed by appropriate secondary antibodies (Alexa Flour 488 and Alexa Flour 546, 1:1000, (Molecular Probes, Carlsbad, CA)) for 1 h at room temperature, and three washes with PBS. The coverslips were inverted and mounted on a slide using Hydromount mounting media. Confocal fluorescence microscopy imaging was performed using Zeiss 510 Meta confocal laser scanning microscope (LSM 510 META). Visualization of the fluorophores was achieved using the 488-nm argon laser, and a 543-nm helium/neon laser.

Measurement of PI Hydrolysis—BV2 microglia, cultured in 96-well plates, were incubated overnight with 0.625 μCi/well myo-[³H]inositol (PerkinElmer Life Sciences) to label the cell membrane phosphoinositides (PIs). After two washes with

A
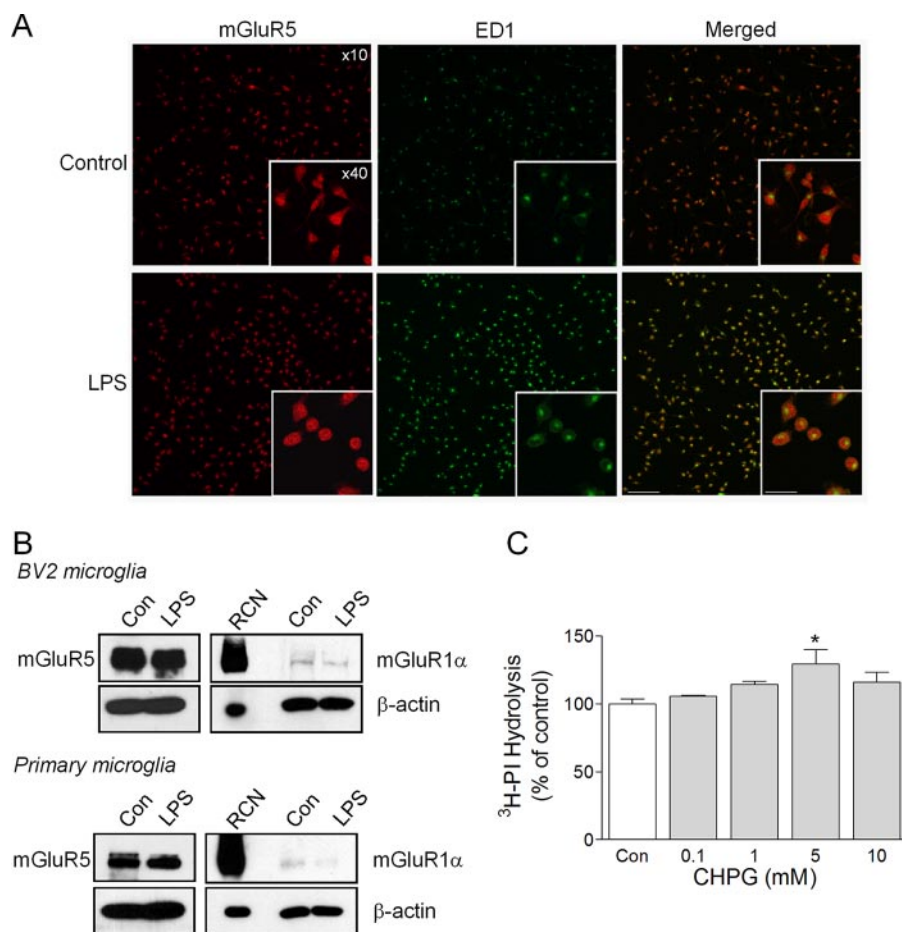
FIGURE 1. **Microglia express functional mGluR5 receptors.** *A*, mGluR5 receptor immunocytochemistry (*red*) revealed strong mGluR5 expression on control- and LPS-stimulated BV2 microglia. LPS stimulation (100 ng/ml) resulted in microglia changing from a ramified to an amoeboid cell morphology and increased ED1 expression (*green*). *Magnification bars*: ×10 view = 100 μm, and ×40 view (*inset*) = 20 μm. *B*, Western immunoblotting confirmed mGluR5 expression in cultured BV2 and primary cortical microglia, whereas mGluR1α expression was weak and negligible by comparison. Rat cortical neuron (*RCN*) samples were run alongside as a positive control for mGluR1α. *C*, the selective mGluR5 agonist, CHPG, stimulated significant phosphoinositide hydrolysis in BV2 microglia (*, $p < 0.05$, *versus* control, ANOVA), thereby demonstrating the presence of a functional mGluR5 receptor. Values represent means ± S.E. from at least five independent measurements.
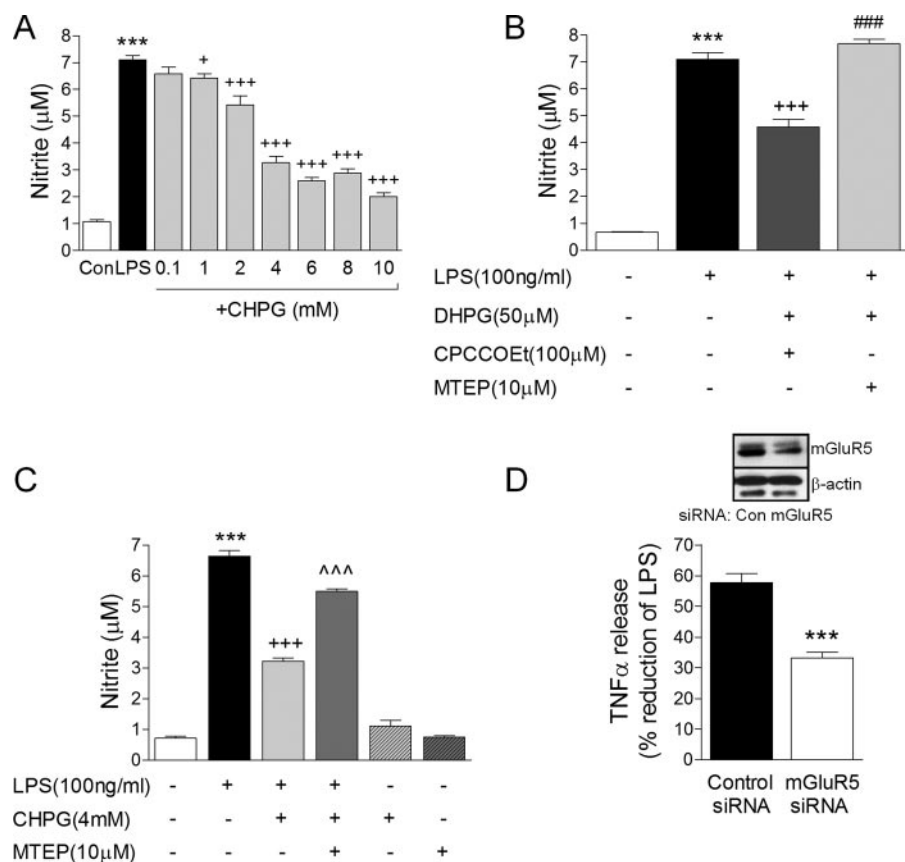
5% CO_2 for the indicated time. Cells were harvested by scraping with a cell scraper and maintained on ice. Samples were washed once with ice-cold PBS and centrifuged at 2,000 × g for 3 min. The cellular pellet was resuspended in lysis buffer (60 mM Tris-HCl, pH 7.8, containing 150 mM NaCl, 5 mM EDTA, 10% glycerol, 2 mM Na_3VO_4, 25 mM NaF, 10 μg/ml leupeptin, 10 μg/ml aprotinin, 1 mM 4-(2-aminoethyl)benzenesulfonylfluoride hydrochloride, 1 mM pepstatin, 1 μM microcystin LR (all Sigma-Aldrich), and 1% Triton X-100 (Calbiochem)). The samples were lysed on ice for 30 min and centrifuged at 20,000 × g for 15 min. The soluble fraction containing total cell extracts was recovered, the protein concentration was determined, and samples were equalized. Protein samples were resolved by 8–15% SDS-PAGE (Mini-Protean 3, Bio-Rad Laboratories), transferred onto nitrocellulose membrane (Optitran BA-S 85, Whatman, Dassel, Germany), and blocked for a minimum of 1 h in blocking buffer (5% skimmed milk in PBS containing 0.05% Tween 20 (PBS-T)). Membranes were incubated overnight at 4 °C with antibodies for mGluR5 (1:1,000, Abcam), mGluR1α (1:1,000, Chemicon International, Billerica, MA), iNOS (1:1,000, BD Transduction Laboratories), p22^{phox} (1:1,000, Santa Cruz Biotechnology), gp91^{phox} (1:1,000, BD Transduction Laboratories), and β-actin (1:10,000, Sigma-Aldrich) in PBS-T containing 1% skimmed milk. Membranes were washed (4 × 10 min in PBS-T), incubated in the appropriate horseradish peroxidase-conjugated secondary antibodies (anti-mouse IgG or anti-rabbit IgG, 1:2,000, Jackson ImmunoResearch) for 1 h at room temperature. Membranes were washed, and protein complexes were visualized using SuperSignal West Dura Extended Duration Substrate (Pierce). Protein immunoblots were exposed to x-ray film (RPI Corp., Mt. Prospect, IL) and processed using a Fuji x-ray processor. Protein bands were quantitated by densitometric analysis using QuantityOne Basic software (Bio-Rad). The data presented represents the density of target protein divided by the density of the endogenous β-actin in each sample, and are expressed in arbitrary units.

Nitric Oxide Assay—NO production was assayed using the Griess Reagent Assay (Invitrogen), according to the manufacturer's instructions.

TNFα Assay—A sandwich enzyme-linked immunosorbent assay was used for detecting TNFα (R&D Systems, Minneapo-

Locke's buffer (156 mM NaCl, 5.6 mM KCl, 3.6 mM NaHCO$_3$, 1 mM MgCl$_2$, 1.3 mM CaCl$_2$, 5.6 mM glucose, and 20 mM Hepes, pH 7.4) incubations with CHPG were carried out for 1 h at 37 °C in Locke's buffer containing 20 mM LiCl to block inositol phosphate degradation. The reaction was terminated by aspiration of media, and inositol phosphates were extracted with 0.1 M HCl for 10 min. The separation of [³H]inositol phosphates was performed by ion-exchange chromatography on AG 1-X8 resin (200–400 mesh, Bio-Rad). The samples were diluted 10 times with water and applied to columns equilibrated in 0.1 M formic acid. The columns were washed with 1 ml of water and 1 ml of tetraborate buffer (5 mM sodium tetraborate, 60 mM sodium formate). Total [³H]inositol phosphates were eluted from the columns with 0.5 ml of 0.1 M formic acid/1 M ammonium formate. The collected samples were mixed with Safety-Solve mixture (RPI, Mount Prospect, IL) and measured by scintillation counting.

Western Immunoblot Analysis—BV2 and primary cortical microglia, cultured in 6-well dishes, were pre-treated for 1 h with CHPG, stimulated with LPS, and incubated at 37 °C and

FIGURE 2. **Selective stimulation of mGluR5 attenuates microglial activation.** *A*, CHPG dose-dependently attenuated LPS-stimulated nitric oxide (NO) production in BV2 microglia. *B*, the group I mGluR agonist, DHPG (50 μM), when applied to microglia in combination with the mGluR1 antagonist, CPCCOEt (100 μM), significantly attenuated LPS-stimulated NO production, whereas DHPG in combination with the mGluR5 antagonist, MTEP (10 μM), failed to modulate LPS-stimulated NO production. *C*, the mGluR5 antagonist, MTEP (10 μM), reversed CHPG attenuation of LPS-stimulated NO production. *D*, CHPG attenuation of LPS-stimulated TNFα production was significantly reduced in mGluR5 siRNA-transfected BV2 microglia when compared with control siRNA-transfected cells. mGluR5 receptor knockdown was confirmed by Western immunoblotting (*inset*, representative immunoblot of three independent experiments). For each of the above BV2 microglia were pretreated with various concentrations of drug for 1 h and stimulated with LPS (100 ng/ml) for 24 h. Values represent means $\pm$ S.E. from at least 6 independent measurements. ***, $p < 0.001$, *versus* control; [+], $p < 0.05$, [+++], $p < 0.001$ *versus* LPS;[###], $p < 0.001$ *versus* LPS+DHPG+CPCCOEt; [^^^], $p < 0.001$ *versus* LPS+CHPG, ANOVA.

lis, MN) in culture supernatants. Assays were performed as per the manufacturer's instructions. Cytokine concentrations were calculated using standard curves generated from recombinant mouse TNFα, and the results were expressed in pg/ml.

Measurement of Intracellular ROS—Intracellular ROS levels were measured by 2′,7′-dichlorodihydrofluorescein diacetate (H$_2$DCFDA). Briefly, BV2 microglia were pre-treated with CHPG (4 mM) or apocynin (1 mM) and stimulated with LPS (100 ng/ml) for 24 h. The cells were incubated with 10 μM H$_2$DCFDA (Molecular Probes, Eugene, OR) for 45 min at 37 °C in 5% CO$_2$. Fluorescence was measured using excitation and emission wavelengths of 490 and 535 nm, respectively. Data are presented as percentage of control-treated values.

NADPH Oxidase Activity Assay—NADPH oxidase activity was assessed using a dihydroethidium-derived fluorescence assay for NADPH oxidase in the microplate reader as previously described (29). Briefly, BV2 microglia, cultured in 6-well plates, were pre-treated with CHPG (4 mM) or apocynin (1 mM) and stimulated with LPS (100 ng/ml) for 4 and 24 h. Cell membrane homogenates were obtained by centrifugation at

18,000 $\times$ *g* for 15 min to separate mitochondria and nuclei, and the supernatant was further centrifuged at 100,000 $\times$ *g* for 1 h to obtain a membrane-enriched fraction. Membrane fractions (10 μg) were incubated with dihydroethidium (10 μM) and DNA (1.25 μg/ml) in PBS/DTPA with the addition of NADPH (50 μM), at a final volume of 120 μl for 30 min at 37 °C in the dark. Fluorescence emissions were followed in a cytofluorometer (excitation 490 nm and emission 590 nm). Data are presented as percentage of control-treated values.

Neurotoxicity Assay—BV2 microglia were pre-treated for 1 h with CHPG (4 mM), stimulated with LPS (100 ng/ml), and incubated at 37 °C and 5% CO$_2$ for 24 h. Conditioned media from BV2 microglia was added to confluent B35 neuroblastoma cells, and the cells were incubated at 37 °C and 5% CO$_2$ for a further 24 h. Cell death was measured by lactate dehydrogenase release assay (CytoTox96[TM] non-radioactive cytotoxicity assay, Promega, Madison, WI) according to the manufacturer's instructions. Neuronal cell death was determined by subtracting the lactate dehydrogenase values in conditioned BV2 media (day 1) from lactate dehydrogenase values in B35 neuroblastoma media (day 2).

Statistical Analysis—For statistical analysis, data obtained from independent measurements are presented as the mean $\pm$ S.E., and they were analyzed using a Student's *t* test or ANOVA followed by the post-hoc Newman-Keuls Multiple Comparison Test. All statistical tests were performed using the GraphPad Prism, Version 3.02 for Windows (GraphPad Software, Inc., San Diego, CA). Differences were considered significant for $p < 0.05$.

RESULTS

Microglia Express Functional mGluR5 Receptors—mGluRs have been identified on microglia and other immune cells, but the functional role of group I mGluRs on microglia have been understudied. To demonstrate the expression of mGluR5 on microglia, immunohistochemical studies using antibodies directed against mGluR5 and ED-1, a marker of activated microglia, were performed on BV2 microglia that had been cultured in the presence or absence of LPS (100 ng/ml) for 24 h. Strong mGluR5 immunolabeling was observed in control- and LPS-stimulated microglia, and LPS treatment transformed the microglia from a predominantly resting, flat cell morphology to
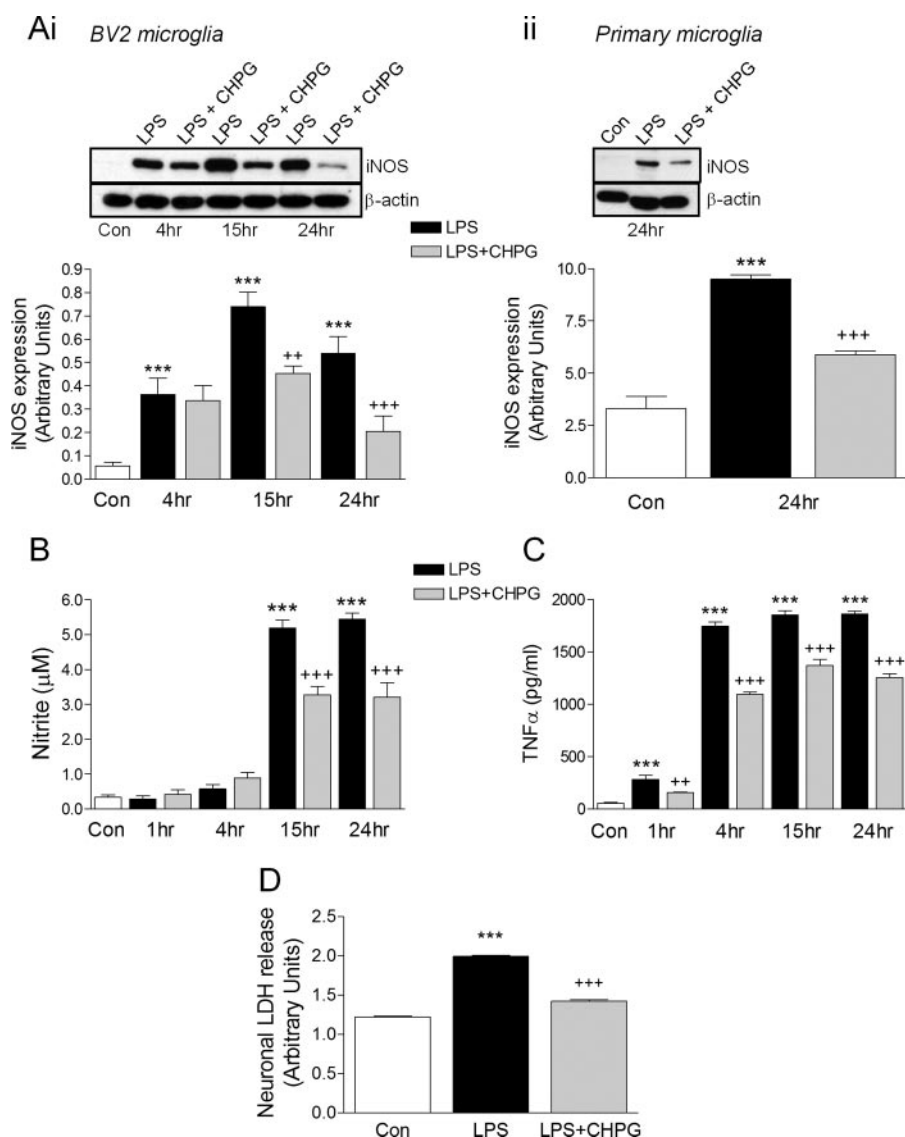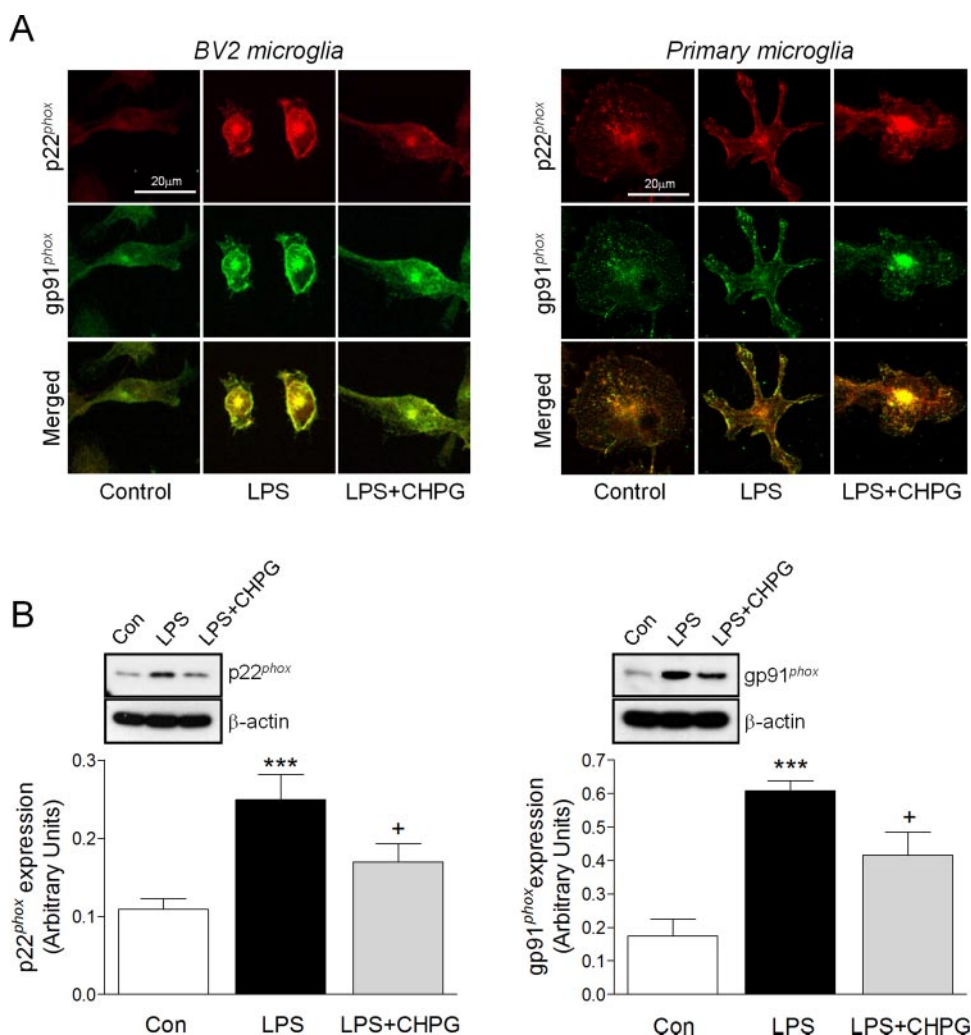
FIGURE 3. mGluR5 activation attenuates the release LPS-stimulated pro-inflammatory mediators and microglial-mediated neurotoxicity. LPS stimulation (100 ng/ml) in BV2 microglia significantly increased iNOS expression at 4, 15, and 24 h (*A, panel i*), NO production at 15 and 24 h (*B*), TNFα production at 1, 4, 15, and 24 h (*C*) (***, $p < 0.001$, *versus* control, ANOVA). Pre-treatment of cells with CHPG (4 mM) significantly attenuated LPS-stimulated increases in each measure at the times indicated ([++], $p < 0.01$, [+++], $p < 0.001$, *versus* LPS, ANOVA). LPS stimulation also increased iNOS expression in primary cortical microglia (*A, panel ii*, ***, $p < 0.001$, *versus* control, ANOVA) and CHPG pre-treatment significantly reduced iNOS expression after 24 h ([+++], $p < 0.001$, *versus* LPS, ANOVA). Conditioned media from LPS-stimulated microglia induced B35 neuroblastoma cell death (***, $p < 0.001$, *versus* control, ANOVA). However, pre-treatment of microglia with CHPG prior to LPS stimulation and addition of conditioned media to neurons resulted in reduced cell death ([+++], $p < 0.001$, *versus* LPS, ANOVA). Values represent means ± S.E. from at least six independent measurements. Representative iNOS immunoblots are shown in (*A, panels i and ii*).

protein kinase C activation, and calcium release. To demonstrate that mGluR5 receptors on microglia are functional, signaling mechanisms downstream of the receptor were assessed. Increasing concentrations of CHPG, a selective mGluR5 agonist, were added to BV2 microglia, and hydrolysis of myo-[³H]inositol was measured after 1 h. CHPG treatment dose-dependently increased PI hydrolysis with a significant increase at 5 mM (Fig. 1*C*, *, $p < 0.05$ *versus* control, ANOVA), demonstrating Gα_q activation and the presence of functional mGluR5 receptors on microglia.

Selective Activation of mGluR5 Reduces Microglial Activation—To determine if mGluR5 stimulation can modulate microglial activation, BV2 microglia were cultured in 96-well plates and mGluR5 agonists/antagonists were added alone or in combination for 1 h, and the cells were subsequently stimulated by LPS for a further 24 h. NO release from microglia was measured as a classic marker of activation. The selective mGluR5 agonist, CHPG, significantly attenuated LPS-stimulated NO production in a dose-dependent manner starting at 1 mM (Fig. 2*A*, [+], $p < 0.05$, [+++], $p < 0.001$ *versus* LPS, ANOVA). 4 mM CHPG reduced LPS-stimulated NO production by ~50%, and this concentration was used for all subsequent experiments. Moreover, a combinatorial pharmacological approach that targeted mGluR5 receptor activation by adding the non-selective group I mGluR agonist DHPG (50 μM) in the presence of a mGluR1 antagonist, CPCCOEt (100 μM), also resulted in significant attenuation of NO production in response to LPS stimulation (Fig. 2*B*, [+++], $p < 0.001$ *versus* LPS, ANOVA). In contrast, combinational pharmacology that targeted mGluR1 (DHPG (50 μM) in the presence of an mGluR5 antagonist, MTEP (10 μM)) did not affect LPS-stimulated NO production in BV2 microglia. In addition, the mGluR5 antagonist MTEP (10 μM) reversed CHPG attenuation of LPS-stimulated NO production when it was added to the cells prior to CHPG pre-treatment (Fig. 2*C*, ^^^, $p < 0.001$ *versus* LPS+CHPG, ANOVA), suggesting that CHPG acts through the mGluR5 receptor. Application of CHPG or MTEP in the absence of LPS did not result in microglial activation or the release of NO (Fig. 2*C*). Furthermore,

an activated, amoeboid-shaped morphology with intensified ED-1 immunoreactivity (Fig. 1*A*). Western immunoblot analysis confirmed that mGluR5 was clearly expressed in BV2 microglia under control- and LPS-stimulated conditions, whereas expression of the other group I mGluR, mGluR1α, was barely detectable in these cells (Fig. 1*B*). Similarly, when the expression of these receptors was assessed in cultured primary cortical microglia, mGluR5 was found to be highly expressed in control and LPS-simulated cortical microglia, whereas mGluR1 expression was weak and negligible by comparison (Fig. 1*B*). Classic activation of mGluR5 receptors results in Gα_q activation, phospholipase C phosphorylation, phosphoinositide (PI) hydrolysis,

FIGURE 4. **mGluR5 activation reduces LPS-stimulated p22^{phox} and gp91^{phox} expression in microglia.** *A*, immunocytochemistry for the NADPH oxidase subunits p22^{phox} (*red*) and gp91^{phox} (*green*) in BV2 and primary cortical microglia, revealed increased expression and membrane co-localization (*merged*) of both subunits in activated microglia after LPS stimulation, which was considerably down-regulated by pre-treatment with CHPG. *Magnification bar* = 20 μm. *B*, Western immunoblotting confirmed that CHPG pre-treatment significantly attenuated p22^{phox} and gp91^{phox} protein expression following LPS stimulation in BV2 microglia (***, $p < 0.001$, *versus* control; +, $p < 0.05$, *versus* LPS, ANOVA). Values represent means ± S.E. from at least six independent measurements. Representative p22^{phox} and gp91^{phox} immunoblots are shown in *B*.

CHPG Attenuates the Release of LPS-stimulated Pro-inflammatory Mediators and Microglial-mediated Neurotoxicity—Upon activation, microglia exert neurotoxic effects by releasing pro-inflammatory mediators such as NO and TNFα. We assessed the time course of microglial activation following LPS stimulation to see if mGluR5 activation modulates the release of pro-inflammatory mediators. Expression of iNOS protein was significantly increased after 4 h of stimulation, peaked at 15 h, and remained elevated through 24 h of stimulation (Fig. 3Ai, ***, $p < 0.001$ *versus* control, ANOVA). Pre-treatment of BV2 microglia with CHPG significantly attenuated the expression of iNOS at 15 and 24 h post-treatment (++, $p < 0.01$, +++, $p < 0.001$ *versus* LPS). iNOS expression was also assessed in primary cortical microglia: LPS stimulation resulted in increased iNOS expression after 24 h that was significantly reduced by CHPG pre-treatment (Fig. 3Aii, ***, $p < 0.001$ *versus* control, +++, $p < 0.001$ *versus* LPS, ANOVA). NO production was monitored over time in BV2 microglia and was significantly elevated after 15 and 24 h stimulation with LPS (Fig. 3B, ***, $p < 0.001$ *versus* control, ANOVA). As anticipated, CHPG pre-treatment resulted in attenuated levels of NO production at both time points (+++, $p < 0.001$ *versus* LPS) thereby demon-

siRNA knockdown of the mGluR5 receptor reduced CHPG's protective effects following LPS stimulation. In BV2 microglia that expressed scrambled control-siRNA, CHPG pre-treatment resulted in a 57.74 ± 2.98% reduction in LPS-stimulated TNFα pro-inflammatory cytokine release (Fig. 2D). In contrast, in BV2 microglia expressing mGluR5-siRNA, CHPG pre-treatment resulted in only a 33.18 ± 1.98% reduction. These data indicate that an approximate 57.46% loss of the effectiveness of CHPG was achieved when the mGluR5 receptor was knocked down in BV2 microglia (Fig. 2D, ***, $p < 0.001$, Student's t test). The incomplete effect of mGluR5-siRNA on the actions of CHPG was due to partial mGluR5 protein knockdown (~50%) probably resulting from a 50% transfection efficiency of siRNA oligonucleotides in BV2 microglia (see "Experimental Procedures"). These data suggest that the mGluR5 receptor mediates the modulatory actions of CHPG in microglia.

strating that mGluR5 activation attenuates NO release from microglia after LPS stimulation. We measured the levels of the pro-inflammatory cytokine, TNFα, over time and observed elevated levels of microglial TNFα release as early as 1 h post stimulation with highest TNFα levels between 4 and 24 h of stimulation (Fig. 3C, ***, $p < 0.001$ *versus* control, ANOVA). CHPG pre-treatment significantly reduced LPS-stimulated TNFα release from microglia as early as 1 h post-treatment through 24-h post-treatment (++, $p < 0.01$, +++, $p < 0.001$ *versus* LPS). Thus, activation of mGluR5 attenuated microglial activation and reduced the release of pro-inflammatory mediators that are known to induce neuronal cell death. Furthermore, when conditioned media from LPS-stimulated microglia was added to cultured B35 neuroblastoma cells, neuronal cell death, as measured by neuronal LDH release, was significantly increased after 24 h (***, $p < 0.001$ *versus* control, ANOVA). However, pre-treatment of

microglia with CHPG prior to LPS stimulation and addition of conditioned media to neurons significantly reduced neuronal cell death ([+++], $p < 0.001$ *versus* LPS), demonstrating the neuroprotective effect of stimulating microglial mGluR5 receptors.

mGluR5 Activation Inhibits Microglial NADPH Oxidase Activity and LPS-generated ROS—ROS generated by NADPH oxidase is an early microglial response to environmental stresses or immunological challenges that often leads to neurotoxicity. Because NADPH oxidase mediates LPS-induced neurotoxicity and pro-inflammatory gene expression in activated microglia (4), we investigated whether mGluR5 activation might modulate microglial NADPH oxidase activity and the subsequent generation of ROS in our model. We first assessed the expression of the membrane subunits of the NADPH oxidase complex, p22^{phox} and gp91^{phox}, following stimulation with LPS for 24 h in BV2 or primary cortical microglia (Fig. 4A). LPS stimulation increased p22^{phox} and gp91^{phox} immunostaining that co-localized at the membrane of activated microglia in BV2 and primary cortical cultures. Pre-treatment of microglia for 1 h with CHPG decreased p22^{phox} and gp91^{phox} immunostaining that was diffusely distributed throughout the cell, similar to control-treated microglia. Quantitative analysis of p22^{phox} and gp91^{phox} expression by Western immunoblotting confirmed a significant increase in p22^{phox} and gp91^{phox} expression after LPS stimulation (Fig. 4B, ***, $p < 0.001$ *versus* Control, ANOVA) that was significantly reduced by pre-treatment with CHPG ([+], $p < 0.05$ *versus* LPS). These data demonstrate that mGluR5 activation down-regulates the expression of the NADPH oxidase components p22^{phox} and gp91^{phox} following LPS stimulation.

The enzymatic activity of NADPH oxidase was assessed in BV2 microglia that were stimulated for 4 or 24 h, with LPS and/or prior pre-treatment with CHPG or the NADPH oxidase inhibitor apocynin (1 mM). LPS caused a significant increase in NADPH oxidase activity after 4 h of stimulation (Fig. 5A, ***, $p < 0.001$ *versus* Control, ANOVA) while pre-treatment with CHPG attenuated the activity of NADPH oxidase, returning it to control levels ([+++], $p < 0.001$ *versus* LPS). Application of the NADPH oxidase inhibitor apocynin prior to LPS stimulation resulted in a comparable reduction in NADPH oxidase activity ([+++], $p < 0.001$ *versus* LPS). Incidentally, NADPH oxidase activity was also increased after 24 h of stimulation, but did not reach statistical significance; both treatments reduced NADPH oxidase activity at this time point (data not shown). Finally, intracellular ROS generation was measured in BV2 microglia via DCFH oxidation. DCFH-DA enters cells passively and is deacetylated by esterase to non-fluorescent DCFH. DCFH reacts with ROS to form dichlorodifluorescein, the fluorescent product. Intracellular ROS was generated in BV2 microglia that had been stimulated with LPS for 24 h (Fig. 5B, ***, $p < 0.001$ *versus* control, ANOVA). Pre-treatment of microglia with CHPG or apocynin caused a significant, comparable reduction in intracellular ROS production in response to LPS stimulation ([++], $p < 0.01$ and [+], $p < 0.05$ *versus* LPS), and application of CHPG or apocynin in the absence of LPS resulted in no ROS generation. Thus, activation of mGluR5 by CHPG reduces p22^{phox} and gp91^{phox} expression and membrane co-localiza-
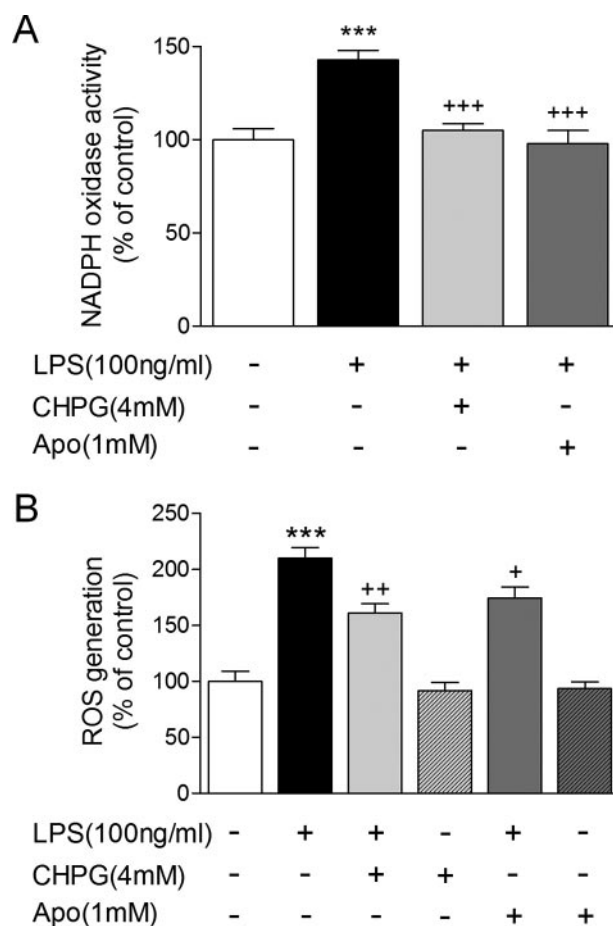
FIGURE 5. **mGluR5 activation inhibits microglial NADPH oxidase activity and intracellular ROS generation.** *A*, LPS stimulation of BV2 microglia resulted in increased microglial NADPH oxidase enzymatic activity after 4 h (***, $p < 0.001$, LPS *versus* control, ANOVA). Pre-treatment of microglia with CHPG or the NADPH oxidase inhibitor, apocynin (1 mM), significantly reduced LPS-stimulated NADPH oxidase activity ([+++], $p < 0.001$, *versus* LPS, ANOVA). *B*, LPS stimulation caused significant intracellular ROS generation in BV2 microglia after 24 h (***, $p < 0.001$, *versus* control, ANOVA). Pre-treatment with CHPG or apocynin, significantly reduced LPS-stimulated ROS production ([+], $p < 0.05$ and [++], $p < 0.01$, *versus* LPS, ANOVA) at this time, whereas neither drug had any effect on its own. Values represent means ± S.E. from at least six independent measurements.

tion, blocks the enzymatic activity of NADPH oxidase complex, and attenuates intracellular ROS generation in microglia following LPS stimulation.

siRNA Knockdown of p22^{phox} and gp91^{phox} Reduces the Protective Effects of mGluR5 Activation—To confirm that inhibition of NADPH oxidase is a key mechanism through which CHPG attenuates microglial activation, we used siRNA to knockdown the expression of NADPH oxidase components p22^{phox} or gp91^{phox}. Western immunoblotting was performed to determine protein knockdown by targeted siRNA: p22^{phox} or gp91^{phox} protein expression was reduced by 52 and 60%, respectively, compared with control siRNA-transfected cell levels (Fig. 6A, *panels i* and *ii*). Because mGluR5 receptor activation by CHPG pre-treatment significantly attenuates LPS-stimulated NO and TNFα release from BV2 microglia (Figs. 2A and 3C), these pro-inflammatory mediators were measured in control-, p22^{phox}-, and gp91^{phox}-siRNA-transfected cells to determine if NADPH oxidase knockdown alters the protective
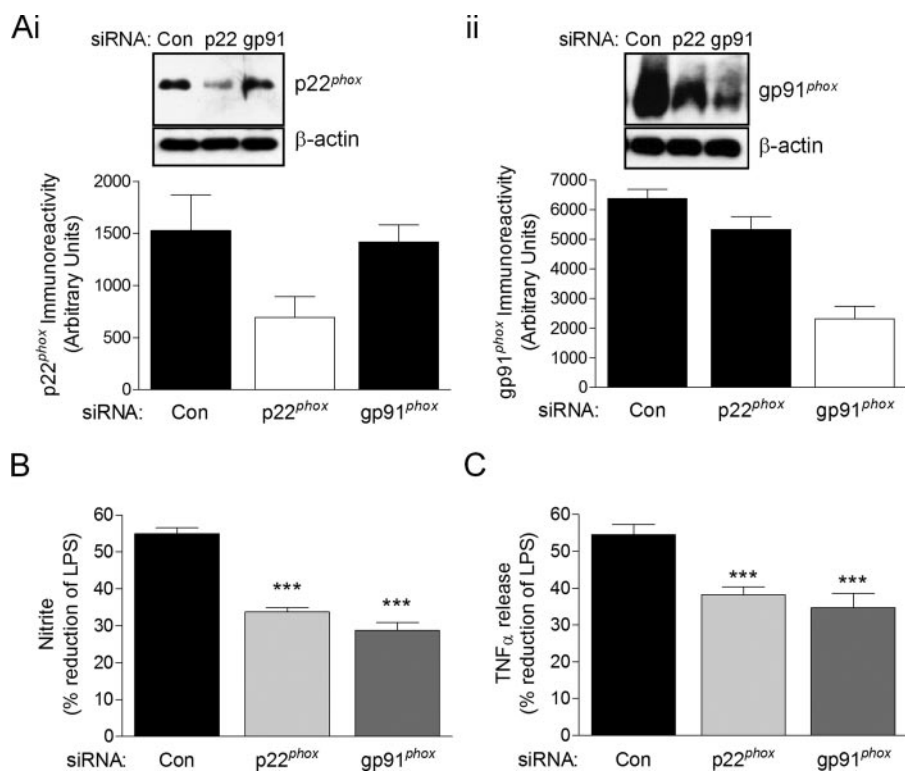
FIGURE 6. **siRNA knockdown of p22^{phox} and gp91^{phox} reduces the protective effects of mGluR5 activation.** *A*, Western immunoblotting demonstrated a 52% reduction in p22^{phox} and 60% reduction in gp91^{phox} protein expression when BV2 microglia were transfected with p22^{phox}-siRNA (*i*) and gp91^{phox}-siRNA (*ii*) as compared with scrambled control-siRNA-transfected cells. Representative immunoblots are shown of six independent measurements. *B*, CHPG attenuation of LPS-stimulated NO production was significantly reduced in p22^{phox}- and gp91^{phox}-siRNA-transfected BV2 microglia when compared with control-siRNA transfected cells (***, $p < 0.001$, *versus* control, ANOVA). *C*, CHPG attenuation of LPS-stimulated TNFα release was significantly reduced in p22^{phox}- and gp91^{phox}-siRNA-transfected BV2 microglia when compared with control-siRNA transfected cells (***, $p < 0.001$, *versus* control, ANOVA). Values represent means ± S.E. from at least six independent measurements.

actions of CHPG. In BV2 microglia that expressed the scrambled control-siRNA, CHPG pre-treatment resulted in a 54.98 ± 1.59% reduction in LPS-stimulated NO release (Fig. 6*B*). In contrast, in BV2 microglia expressing p22^{phox}- or gp91^{phox}-siRNA, CHPG pre-treatment caused a 33.76 ± 1.22% and 28.73 ± 2.22% reduction, respectively. Similarly, CHPG pre-treatment in control-siRNA microglia resulted in a 54.52 ± 2.82% reduction in LPS-stimulated TNFα release (Fig. 6*C*), whereas CHPG treatment in p22^{phox}- or gp91^{phox}-siRNA microglia resulted in a 38.28 ± 2.04% and 34.73 ± 3.88% reduction in TNFα release, respectively. These data indicate that a reduction in NADPH oxidase membrane subunits p22^{phox} or gp91^{phox} by between 50 and 60% results in an approximate 38% loss of the effectiveness of CHPG. These data suggest that a key mechanism through which CHPG reduces microglial activation, and the release of pro-inflammatory mediators is by directly inhibiting the NADPH oxidase complex.

mGluR5 Stimulation Also Attenuates IFNγ-dependent Microglial Activation—To determine if CHPG's modulatory effects on microglia were unique for LPS stimulation an alternative central nervous system immuno-activator was tested. The pro-inflammatory cytokine, IFNγ, stimulates microglial activity (5) and participates in microglial-mediated neurotoxicity (30). BV2 microglia were pre-treated with CHPG (4 mM) for

1 h and subsequently stimulated with increasing concentrations of IFNγ (0.5 and 2 ng/ml) for a further 24 h. IFNγ dose-dependently stimulated the production of NO (Fig. 7*A*, ***, $p < 0.001$ *versus* control, ANOVA), while CHPG pre-treatment reduced IFNγ-stimulated NO production by more than 50% at both concentrations (+++, $p < 0.001$ *versus* IFNγ, ANOVA). Similarly, IFNγ-stimulated microglia released increasing concentrations of TNFα (Fig. 7*B*, ***, $p < 0.001$ *versus* control, ANOVA). In contrast, CHPG pre-treatment prevented IFNγ-stimulated TNFα release in microglia (+++, $p < 0.001$ *versus* IFNγ, ANOVA), demonstrating that microglial activation induced by another physiologically relevant immunostimulator was significantly attenuated by mGluR5 activation. Taken together, the LPS and IFNγ studies suggest that mGluR5 activation suppresses key pro-inflammatory signaling pathways that are involved in microglial-mediated neurodegeneration.

DISCUSSION

In addition to their expression on neurons, mGluRs are expressed on other cells, including microglia, macrophages, astrocytes, and lymphocytes (17, 18, 20, 21, 31, 32). In this study we used an established murine microglial cell-line (BV2 microglia) to investigate the modulatory role of microglial mGluR5 receptor activation and confirmed key observations in cultured primary cortical microglia. We demonstrate that mGluR5 is expressed in cultured microglia, whereas the other group I mGluR, mGluR1, is minimally expressed; this profile is consistent with the previous report of mGluR5 mRNA expression in microglia (19). Importantly, microglial mGluR5 receptors are functional as demonstrated by phosphoinositide hydrolysis and activation of the classical signaling pathways when stimulated by the selective mGluR5 agonist CHPG. Activation of mGluR5 negatively regulates the release of microglial associated inflammatory mediators in response to the bacterial endotoxin LPS and the pro-inflammatory cytokine IFNγ. Moreover, mGluR5 activation prevents microglial-mediated neuronal cell death. To verify that these effects were mediated by the mGluR5 receptor, rather than a non-receptor related mechanism, we demonstrated that CHPG effects were markedly reduced by a selective mGluR5 receptor antagonist or by protein knockdown using siRNA. Furthermore, we propose that the protective effects of mGluR5 activation are mediated by the inhibition of microglial NADPH oxidase complex because CHPG blocked NADPH oxidase
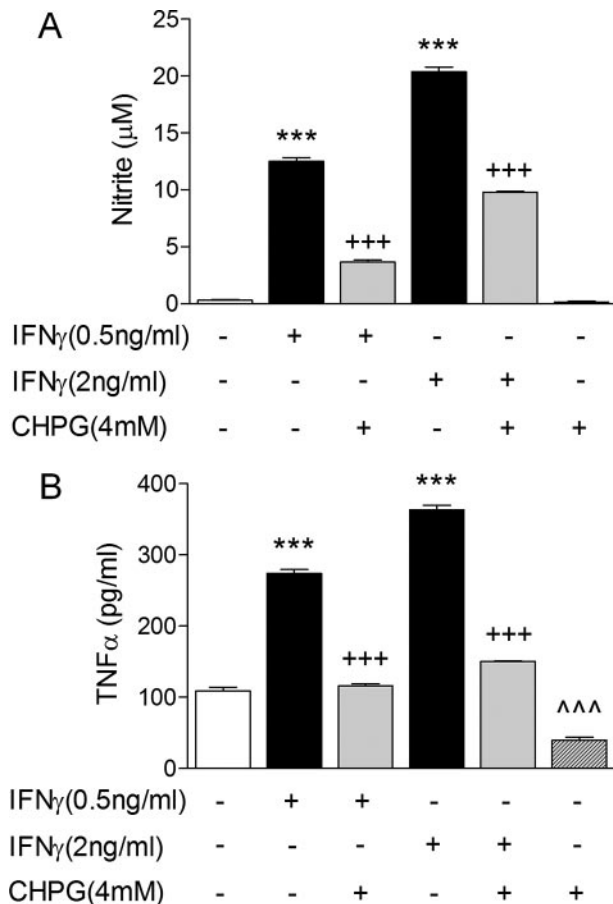
FIGURE 7. mGluR5 activation attenuates IFNγ-stimulated microglial activation and the release of pro-inflammatory mediators. BV2 microglia were pre-treated with CHPG (4 mM) for 1 h and stimulated with increasing concentrations of IFNγ (0.5 and 2 ng/ml) for a further 24 h. *A*, IFNγ dose-dependently stimulated the production of NO in microglia (***, $p < 0.001$ *versus* control, ANOVA), while CHPG pre-treatment significantly attenuated IFNγ-stimulated NO production ($^{+++}$, $p < 0.001$ *versus* IFNγ, ANOVA). *B*, IFNγ dose-dependently stimulated the release of increasing concentrations of TNFα from microglia (***, $p < 0.001$ *versus* control, ANOVA), whereas CHPG pre-treatment significantly attenuated IFNγ-stimulated TNFα release ($^{+++}$, $p < 0.001$ *versus* IFNγ, ANOVA). Values represent means ± S.E. from at least six independent measurements.

enzymatic activity and reduced the expression of its membrane subunits p22^{phox} and gp91^{phox}. In addition, the protective effects of CHPG were significantly reduced when the p22^{phox} or gp91^{phox} subunits of NADPH oxidase complex were knocked down by siRNA.

The pro-inflammatory mediators NO and TNFα have been shown to contribute to neuronal damage and death *in vitro* and *in vivo* (22, 33–35). NO is associated with neuronal cell death through the production of the toxic metabolite peroxynitrite or via direct actions on mitochondrial and cellular lipid membranes (36, 37). High levels of NO induce neuronal death by inhibiting mitochondrial cytochrome oxidase and neuronal respiration, causing depolarization and glutamate release followed by excitotoxicity via *N*-methyl-D-aspartic acid receptors (38–40). In this study, we show that stimulation of microglial mGluR5 receptors using two pharmacological approaches (CHPG and DHPG/CPCCOEt combination) attenuates LPS-stimulated NO production by inhibiting the expression of iNOS. In addition, mGluR5 receptor activation by CHPG sig-

nificantly suppresses the release of TNFα, a powerful pro-inflammatory mediator that stimulates many neuroinflammatory cascades. TNFα can also cause cell death directly by binding to neuronal TNFα receptors linked to death domains that activate caspase-dependent apoptosis (41) or by potentiating glutamate release by blockade of glutamate transporter activity, thereby enhancing excitotoxicity (35). Finally, TNFα also drives self-propagating cycles of microglial activation and neuroinflammation by inducing microglial NADPH oxidase activity and additional release of O^{2-} and superoxide-derived oxidants (42).

Superoxide and its downstream products are highly reactive, and excessive production of free radicals damages cellular proteins, lipids, and DNA, leading to cell death (10). Neurons are vulnerable to oxidative stress and oxidative damage appears to contribute to neuronal cell death in a number of neurodegenerative disease (3). NADPH oxidase has been implicated in the neurotoxic mechanisms of dopaminergic neurotoxic compounds (*e.g.* 1-methyl-4-phenyl-1,2,3,6-tetrahydropyridine, rotenone, and paraquat), aggregated proteins (*e.g.* α-synuclein and β-amyloid), environmental toxins (*e.g.* nanometer-size diesel particles), and inflammogens (*e.g.* LPS) (4, 43–48). These toxins are thought to contribute to the pathogenesis of numerous neurodegenerative diseases; as such over-activated microglial NADPH oxidase likely plays a key role in inflammation-mediated neurodegeneration. We show that mGluR5 activation inhibited NADPH oxidase activity following 4 h of LPS stimulation in a manner similar to the direct inhibition of the NADPH oxidase complex by apocynin. Furthermore, mGluR5 activation down-regulated the expression of the NADPH oxidase membrane components p22^{phox} and gp91^{phox} following LPS stimulation. We propose that this may be a key mechanism of mGluR5's actions, because siRNA knockdown of p22^{phox} or gp91^{phox} significantly reduced the protective effects of stimulating microglial mGluR5 receptors. An outcome of these actions is a significant reduction of intracellular ROS generation in response to LPS, which under normal hyperactive conditions would lead to self-propagating microglial activation and further release of inflammatory mediators. The effects of microglial mGluR5 receptor activation reduces B35 neuroblastoma cell death following LPS stimulation; most probably resulting from the inhibition of NADPH oxidase and pro-inflammatory mediators such as iNOS and TNFα, which are neurotoxic (37, 38, 49). NADPH oxidase-derived ROS has been shown to mediate the effects of LPS and IFNγ on the expression of iNOS and pro-inflammatory cytokines in microglia (5, 50). Furthermore, NADPH oxidase inhibition blocks MAPK, NFκB, and STAT1 signaling pathways, thereby modulating transcription factor activation and gene expression (5). Thus, the protective effects of mGluR5 activation in microglia may reflect, in part, inhibition of NADPH oxidase-derived ROS generation and the subsequent reduced expression of pro-inflammatory mediators and neurotoxic substances.

Other mGluR receptors expressed on microglia may also modulate microglial-mediated neurotoxicity. Activation of microglial group III mGluRs by L-(+)-2-amino-4-phosphonobutyric acid or (*RS*)-4-phosphophenylglycine reduces neurotoxicity after microglial stimulation with LPS and chromogranin A (20). Another report confirmed the protective effects of

group III mGluR activation in a model of myelin-induced microglial neurotoxicity; interestingly, they found that activation of the group II receptor mGluR3 was neuroprotective, whereas activation of mGluR2 exacerbated myelin-induced microglial neurotoxicity (51). This sub-type specific response is also apparent in astrocyte-neuronal cultures, where mGluR3 activation confers protection while mGluR2 activation may be harmful to neurons (52). In neurons, the same is true for group I mGluRs. mGluR1 agonists exacerbate necrotic cell death (23) and selective antagonists are neuroprotective (16, 26, 27), whereas mGluR5 activation inhibits caspase-dependent neuronal apoptosis and appears to provide neuroprotection in animal studies (24). The present findings suggest that the neuroprotective effects of CHPG may also reflect mGluR5 receptor-mediated attenuation of microglial activation; when coupled with its anti-apoptotic effects on neurons, such treatment may have powerful multipotential neuroprotective actions (for review see Ref. 53).

Short term mGluR5 activation can have long lasting neuroprotective effects. For example, in a rat model of focal cerebral ischemia CHPG administration reduced the infarct volume and improved neurological function at 24 h after middle cerebral artery occlusion/reperfusion (54). More recently we have shown that CHPG treatment improves functional motor recovery, reduces lesion volume, and increases white matter sparing at 28 days after spinal cord injury (55). Furthermore, short term administration of CHPG significantly attenuated microglial activation and dose-dependently reduced the release of microglial-derived neurotoxic mediators. Uncontrolled microglial-mediated inflammation and related neuronal damage appears to propagate a positive feedback loop that leads to progressive microglial activation/neuronal loss, which may contribute to the chronic progression of neurodegenerative diseases such Alzheimer and Parkinson diseases (1). Given that microglial-mediated inflammation and apoptotic neuronal cell death have each been implicated in neurodegeneration, mGluR5 may be a promising target for the treatment of both acute central nervous system injury and chronic neurodegenerative disorders.

REFERENCES

1. Gao, H. M., and Hong, J. S. (2008) *Trends Immunol.* **29,** 357–365
2. Hanisch, U. K., and Kettenmann, H. (2007) *Nat. Neurosci.* **10,** 1387–1394
3. Block, M. L., Zecca, L., and Hong, J. S. (2007) *Nat. Rev. Neurosci.* **8,** 57–69
4. Qin, L., Liu, Y., Wang, T., Wei, S. J., Block, M. L., Wilson, B., Liu, B., and Hong, J. S. (2004) *J. Biol. Chem.* **279,** 1415–1421
5. Pawate, S., Shen, Q., Fan, F., and Bhat, N. R. (2004) *J. Neurosci. Res.* **77,** 540–551
6. Cross, A. R., and Segal, A. W. (2004) *Biochim. Biophys. Acta* **1657,** 1–22
7. Choi, S. H., Lee, D. Y., Kim, S. U., and Jin, B. K. (2005) *J. Neurosci.* **25,** 4082–4090
8. Bey, E. A., Xu, B., Bhattacharjee, A., Oldfield, C. M., Zhao, X., Li, Q., Subbulakshmi, V., Feldman, G. M., Wientjes, F. B., and Cathcart, M. K. (2004) *J. Immunol.* **173,** 5730–5738
9. Zhao, X., Xu, B., Bhattacharjee, A., Oldfield, C. M., Wientjes, F. B., Feldman, G. M., and Cathcart, M. K. (2005) *J. Leukoc. Biol.* **77,** 414–420
10. Patel, M., Li, Q. Y., Chang, L. Y., Crapo, J., and Liang, L. P. (2005) *J. Neurochem.* **92,** 123–131
11. Zhang, D., Hu, X., Wei, S. J., Liu, J., Gao, H., Qian, L., Wilson, B., Liu, G., and Hong, J. S. (2008) *J. Neuroinflamm.* **5,** 21
12. Qian, L., Xu, Z., Zhang, W., Wilson, B., Hong, J. S., and Flood, P. M. (2007) *J. Neuroinflamm.* **4,** 23
13. Lea, P. M., 4th, and Faden, A. I. (2006) *CNS Drug Rev.* **12,** 149–166
14. Movsesyan, V. A., and Faden, A. I. (2006) *J. Neurotrauma* **23,** 117–127
15. Faden, A. I., Ivanova, S. A., Yakovlev, A. G., and Mukhin, A. G. (1997) *J. Neurotrauma* **14,** 885–895
16. Faden, A. I., O'Leary, D. M., Fan, L., Bao, W., Mullins, P. G., and Movsesyan, V. A. (2001) *Exp. Neurol.* **167,** 435–444
17. D'Antoni, S., Berretta, A., Bonaccorso, C. M., Bruno, V., Aronica, E., Nicoletti, F., and Catania, M. V. (2008) *Neurochem. Res.* **33,** 2436–2443
18. Schools, G. P., and Kimelberg, H. K. (1999) *J. Neurosci. Res.* **58,** 533–543
19. Biber, K., Laurie, D. J., Berthele, A., Sommer, B., Tölle, T. R., Gebicke-Härter, P. J., van Calker, D., and Boddeke, H. W. (1999) *J. Neurochem.* **72,** 1671–1680
20. Taylor, D. L., Diemel, L. T., and Pocock, J. M. (2003) *J. Neurosci.* **23,** 2150–2160
21. Taylor, D. L., Diemel, L. T., Cuzner, M. L., and Pocock, J. M. (2002) *J. Neurochem.* **82,** 1179–1191
22. Taylor, D. L., Jones, F., Kubota, E. S., and Pocock, J. M. (2005) *J. Neurosci.* **25,** 2952–2964
23. Allen, J. W., Knoblach, S. M., and Faden, A. I. (2000) *Cell Death Diff.* **7,** 470–476
24. Movsesyan, V. A., Stoica, B. A., and Faden, A. I. (2004) *J. Neurochem.* **89,** 1528–1536
25. Lea, P. M., 4th, Movsesyan, V. A., and Faden, A. I. (2005) *Br. J. Pharmacol.* **145,** 527–534
26. Fei, Z., Zhang, X., Bai, H. M., Jiang, X. F., and Wang, X. L. (2006) *J. Clin. Neurosci.* **13,** 1023–1027
27. Szydlowska, K., Kaminska, B., Baude, A., Parsons, C. G., and Danysz, W. (2007) *Eur. J. Pharmacol.* **554,** 18–29
28. Byrnes, K. R., Garay, J., Di Giovanni, S., De Biase, A., Knoblach, S. M., Hoffman, E. P., Movsesyan, V., and Faden, A. I. (2006) *Glia* **53,** 420–433
29. Fernandes, D. C., Wosniak, J., Jr., Pescatore, L. A., Bertoline, M. A., Liberman, M., Laurindo, F. R., and Santos, C. X. (2007) *Am. J. Physiol. Cell Physiol.* **292,** C413–422
30. Mount, M. P., Lira, A., Grimes, D., Smith, P. D., Faucher, S., Slack, R., Anisman, H., Hayley, S., and Park, D. S. (2007) *J. Neurosci.* **27,** 3328–3337
31. Geurts, J. J., Wolswijk, G., Bö, L., van der Valk, P., Polman, C. H., Troost, D., and Aronica, E. (2003) *Brain* **126,** 1755–1766
32. Pacheco, R., Ciruela, F., Casadó, V., Mallol, J., Gallart, T., Lluis, C., and Franco, R. (2004) *J. Biol. Chem.* **279,** 33352–33358
33. He, Y., Imam, S. Z., Dong, Z., Jankovic, J., Ali, S. F., Appel, S. H., and Le, W. (2003) *J. Neurochem.* **86,** 1338–1345
34. Iravani, M. M., Kashefi, K., Mander, P., Rose, S., and Jenner, P. (2002) *Neuroscience* **110,** 49–58
35. Zou, J. Y., and Crews, F. T. (2005) *Brain Res.* **1034,** 11–24
36. Gibbons, H. M., and Dragunow, M. (2006) *Brain Res.* **1084,** 1–15
37. Mander, P., and Brown, G. C. (2005) *J. Neuroinflamm.* **2,** 20
38. Bal-Price, A., and Brown, G. C. (2001) *J. Neurosci.* **21,** 6480–6491
39. Golde, S., Chandran, S., Brown, G. C., and Compston, A. (2002) *J. Neurochem.* **82,** 269–282
40. McNaught, K. S., and Brown, G. C. (1998) *J. Neurochem.* **70,** 1541–1546
41. Zhao, X., Bausano, B., Pike, B. R., Newcomb-Fernandez, J. K., Wang, K. K., Shohami, E., Ringger, N. C., DeFord, S. M., Anderson, D. K., and Hayes, R. L. (2001) *J. Neurosci. Res.* **64,** 121–131
42. Li, J. M., Fan, L. M., Christie, M. R., and Shah, A. M. (2005) *Mol. Cell. Biol.* **25,** 2320–2330
43. Block, M. L., Wu, X., Pei, Z., Li, G., Wang, T., Qin, L., Wilson, B., Yang, J., Hong, J. S., and Veronesi, B. (2004) *FASEB J.* **18,** 1618–1620
44. Gao, H. M., Liu, B., and Hong, J. S. (2003) *J. Neurosci.* **23,** 6181–6187
45. Gao, H. M., Liu, B., Zhang, W., and Hong, J. S. (2003) *FASEB J.* **17,** 1954–1956
46. Qin, L., Liu, Y., Cooper, C., Liu, B., Wilson, B., and Hong, J. S. (2002)

J. Neurochem. **83,** 973–983

47. Wu, X. F., Block, M. L., Zhang, W., Qin, L., Wilson, B., Zhang, W. Q., Veronesi, B., and Hong, J. S. (2005) *Antioxid. Redox Signal.* **7,** 654–661

48. Zhang, W., Dallas, S., Zhang, D., Guo, J. P., Pang, H., Wilson, B., Miller, D. S., Chen, B., Zhang, W., McGeer, P. L., Hong, J. S., and Zhang, J. (2007) *Glia* **55,** 1178–1188

49. Li, J., Baud, O., Vartanian, T., Volpe, J. J., and Rosenberg, P. A. (2005) *Proc. Natl. Acad. Sci. U. S. A.* **102,** 9936–9941

50. Chéret, C., Gervais, A., Lelli, A., Colin, C., Amar, L., Ravassard, P., Mallet, J., Cumano, A., Krause, K. H., and Mallat, M. (2008) *J. Neurosci.* **28,** 12039–12051

51. Pinteaux-Jones, F., Sevastou, I. G., Fry, V. A., Heales, S., Baker, D., and Pocock, J. M. (2008) *J. Neurochem.* **106,** 442–454

52. Corti, C., Battaglia, G., Molinaro, G., Riozzi, B., Pittaluga, A., Corsi, M., Mugnaini, M., Nicoletti, F., and Bruno, V. (2007) *J. Neurosci.* **27,** 8297–8308

53. Byrnes, K. R., Loane, D. J., and Faden, A. I. (2009) *Neurotherapeutics* **6,** 94–107

54. Bao, W. L., Williams, A. J., Faden, A. I., and Tortella, F. C. (2001) *Brain Res.* **922,** 173–179

55. Byrnes, K. R., Stoica, B., Riccio, A., Pajoohesh-Ganji, A., Loane, D. J., and Faden, A. I. (March 26, 2009) *Ann. Neurol.* 10.1002/ana.21673